Targeting Histone Chaperone FACT Complex Overcomes 5-Fluorouracil Resistance in Colon Cancer

Heyu Song[1], Jiping Zeng[1], Shrabasti Roychoudhury[1], Pranjal Biswas[1], Bhopal Mohapatra[1], Sutapa Ray[2], Kayvon Dowlatshahi[3], Jing Wang[4], Vimla Band[1,5], Geoffrey Talmon[3], and Kishor K. Bhakat[1,5]

ABSTRACT

Fluorouracil (5-FU) remains a first-line chemotherapeutic agent for colorectal cancer. However, a subset of colorectal cancer patients who have defective mismatch-repair (dMMR) pathway show resistance to 5-FU. Here, we demonstrate that the efficacy of 5-FU in dMMR colorectal cancer cells is largely dependent on the DNA base excision repair (BER) pathway. Downregulation of APE1, a key enzyme in the BER pathway, decreases IC_{50} of 5-FU in dMMR colorectal cancer cells by 10-fold. Furthermore, we discover that the facilitates chromatin transcription (FACT) complex facilitates 5-FU repair in DNA via promoting the recruitment and acetylation of APE1 (AcAPE1) to damage sites in chromatin. Downregulation of FACT affects 5-FU damage repair in DNA and sensitizes dMMR colorectal cancer cells to 5-FU. Targeting the FACT complex with curaxins, a class of small molecules, significantly improves the 5-FU efficacy in dMMR colorectal cancer *in vitro* (~50-fold decrease in IC_{50}) and *in vivo* xenograft models. We show that primary tumor tissues of colorectal cancer patients have higher FACT and AcAPE1 levels compared with adjacent nontumor tissues. Additionally, there is a strong clinical correlation of FACT and AcAPE1 levels with colorectal cancer patients' response to chemotherapy. Together, our study demonstrates that targeting FACT with curaxins is a promising strategy to overcome 5-FU resistance in dMMR colorectal cancer patients.

Introduction

Colorectal cancer is the second leading cause of cancer-related deaths in the United States. According to the American Cancer Society, more than 50% of new cases are diagnosed at advanced stages and require adjuvant chemotherapy. The pyrimidine analogue 5-fluorouracil (5-FU) forms the backbone for almost all chemotherapeutic regimens for colorectal cancer (1). However, a subset of colorectal cancer patients who develop cancer with microsatellite instability or defective mismatch repair (dMMR) show resistance to 5-FU (2, 3). Studies have shown that dMMR colorectal cancer patients with stage III tumors do not benefit from 5-FU–based adjuvant (FOLFOX) therapy (2, 4). In accordance with clinical observations, *in vitro* studies have shown that dMMR colorectal cancer cells are resistant to the cytotoxic effects of 5-FU (5). Therefore, elucidating the mechanisms of 5-FU resistance in dMMR colorectal cancer and identifying novel therapeutic targets to increase the efficacy of 5-FU in dMMR colorectal cancer represents an unmet need.

Though the mechanism of actions of 5-FU is not completely understood, its cytotoxicity has been ascribed to the inhibition of thymidylate synthase (TS), the key enzyme of *de novo* pyrimidine biosynthesis (6). However, numerous studies have established that 5-FU metabolites can induce cytotoxicity through incorporation into RNA and genomic DNA (7, 8), and that both DNA mismatch repair (MMR) and base excision repair (BER) pathways are primarily involved in the repair of the resultant DNA lesions (8, 9). In the case of FU incorporation opposite dG, the resulting FU:dG mispair would be efficiently processed by the MMR pathway, resulting in single-stranded breaks (SSB; refs. 9, 10). However, repeated incorporation of FU:dG leads to futile attempts by the MMR system and persistent SSBs will result in double-strand breaks that in turn induce apoptosis (11). On the other hand, the BER pathway is able to directly remove FU from newly synthesized DNA in the case of FU:dA or FU:dG (8, 12), resulting in apurinic/apyrimidinic (AP) sites that are further processed by AP-endonuclease (APE1; ref. 13). APE1 plays a central role in the BER pathway by cleaving the DNA backbone immediately 5′ to lesions (14). The resulting strand breaks are repaired via the highly coordinated BER pathway (15). We have recently shown that APE1 is acetylated (AcAPE1) at AP sites in chromatin by p300 and that acetylation enhances its AP-endonuclease activity (16). We hypothesize that dMMR colorectal cancer cells have an increased requirement of the BER pathway for the efficient repair of 5-FU–induced DNA damages, and that targeting the APE1-dependent BER pathway will sensitize dMMR colorectal cancer to 5-FU.

In this study, we sought to examine the role of the BER pathway in promoting 5-FU resistance in colorectal cancer cells with a deficient MMR system. We found that downregulation of APE1 sensitizes dMMR colorectal cancer cells to 5-FU *in vitro*. Furthermore, we identified the facilitates chromatin transcription (FACT) complex as an interacting partner of APE1 in chromatin and characterized the role of the FACT complex in the BER pathway. Curaxins, a class of small molecules that inhibit FACT complex, were tested extensively in combination with 5-FU using multiple dMMR colorectal cancer cell lines *in vitro* and *in vivo* as a means of improving 5-FU therapeutic response. To provide further support of the potential applicability of this novel therapeutic strategy, we examined the expression of APE1 and FACT in colorectal cancer patient specimens and correlated with

[1]Department of Genetics, Cell Biology and Anatomy, University of Nebraska Medical Center, Omaha, Nebraska. [2]Department of Pediatrics, University of Nebraska Medical Center, Omaha, Nebraska. [3]Department of Pathology and Microbiology, University of Nebraska Medical Center, Omaha, Nebraska. [4]Eppley Institute for Cancer Research, University of Nebraska Medical Center, Omaha, Nebraska. [5]Fred & Pamela Buffett Cancer Center, University of Nebraska Medical Center, Omaha, Nebraska.

Note: Supplementary data for this article are available at Molecular Cancer Therapeutics Online (http://mct.aacrjournals.org/).

Corresponding Author: Kishor K. Bhakat, University of Nebraska Medical Center, Omaha, NE 68198. Phone: 402-559-8467; Fax: 402-559-7328; E-mail: kishor.bhakat@unmc.edu

Mol Cancer Ther 2020;19:258–69

doi: 10.1158/1535-7163.MCT-19-0600

the treatment response. Together, our study unveils a novel role of the FACT complex in promoting 5-FU resistance and demonstrates that targeting FACT with curaxins is a promising strategy to overcome 5-FU resistance in dMMR colorectal cancer patients.

Materials and Methods

Cell culture, plasmids, siRNAs, transfection, and treatments

HCT116 cells (ATCC# CCL-247) were grown in McCoy's 5A medium (Gibco) supplemented with 10% fetal calf serum (FCS; Sigma) and antibiotic mixture of 100 U/mL penicillin and 100 μg/mL streptomycin (Gibco). The HCT116 cell line stably expressing APE1-shRNA was a kind gift from Dr. Sheila Crowe (University of California, San Diego) and was cultured in McCoy's 5A supplemented with 0.01% puromycin (Gibco). HEK-293T cells (ATCC; #CRL-3216) were cultured in DMEM-high glucose medium (Gibco) with 10% FCS (Sigma) and antibiotic mixture of 100 U/mL penicillin and 100 μg/mL streptomycin (Gibco). The RKO cell line was obtained from Dr. Jing Wang [Eppley Institute, University of Nebraska Medical Center (UNMC)]. RKO and DLD-1 cells (ATCC# CCL-221) were grown in the EMEM medium (ATCC). All cell lines were authenticated using STR DNA profiling by Genetica DNA Laboratories 2 years ago before being used in this study. These cells were routinely assayed for *Mycoplasma*. Mutation of Lys residue (K6, 7, 27, 31, and 32) to arginine or to glutamine in APE1-FLAG–tagged pCMV5.1 plasmid were generated using a site-directed mutagenesis kit (Agilent-Stratagene) as described previously (16). Exponentially growing HEK293T cells were transfected with wild-type (WT) APE1, K6,7,27,31,32 to arginine (K5R) or to glutamine (K5Q), N-terminal 33 amino acid deleted (NΔ33) mutants expression plasmids. siRNAs targeting SSRP1 (Sigma, EHU015991) and SPT16 (Sigma, EHU039881; Dharmacon, J-009517), as well as control siRNA (Dharmacon, D-001810) were transfected into RKO, HCT116, and HCT116^{APE1shRNA}. APE1 siRNAs were obtained from Sigma-Aldrich (WD04424567) and Dharmacon (J-010237). Cells were transfected using Lipofectamine 2000 (Invitrogen) and harvested after 48 hours. Methyl Methanesulfonate (MMS), quinacrine (QC), and 5-FU were obtained from Sigma-Aldrich. CBL0137 was obtained from Cayman Chemical for *in vitro* study and from Incuron Inc for *in vivo* study.

Identification of interacting proteins of AcAPE1

Chromatin extracts were immunoprecipitated (IP) with anti-AcAPE1 and control IgG antibodies (16). The IP samples were boiled for 5 minutes and resolved in 12.5 % SDS-PAGE gel followed by staining with Coomassie blue (PageBlue, Thermo Scientific). Identification of protein bands was performed by MALDI-TOF-TOF analysis in the Mass Spectrometry and Proteomics Core Facility (UNMC, Omaha, NE).

Western blot analysis

Cell fractionation was performed as described previously (17). Whole-cell lysates or cell fractions were resolved on 10% to 12.5 % SDS-PAGE gel and transferred to nylon membranes for blotting. Whole-cell lysates of HCEC, GEO, LoVo, and SW620 were provided by Dr. Jing Wang (UNMC). Primary antibodies were used, including SPT16 (Abcam, 204343), SSRP1 (BioLegend, 609702), FLAG (Sigma, F1804), TRF1 (Abcam, 10579), α-HSC70 (B6-Sc7298, Santa Cruz Biotechnology), H2A (Abcam, 26350), APE1 (Novus Biologicals, NB100-116), α-tubulin (Abcam, 52666), and AcAPE1 (14, 18). Immunoblot signals were detected using Super Signal West pico chemiluminescent substrate (Thermo Scientific) after treating with HRP-conjugated secondary Ab (GE Healthcare).

MTT assay

Cells were seeded at a density of 5×10^3 in 96-well plates. After 24-hour incubation in the medium to allow for cell attachment, the fresh medium was added and cells were treated with vehicle control (DMSO alone) or indicated doses of 5-FU dissolved in DMSO for 72 hours. The MTT reagent (Sigma-Aldrich, M5655) was added to a final concentration of 0.5 mg/mL to each well. The assay was performed as per the manufacture's protocol. Three independent experiments with six replicates were performed for each group.

Patient tissue samples and analysis

Colon cancer samples were obtained from tissue bank at UNMC and University of Texas Medical Branch. Tissues were collected in accordance with institution's review board approval, and informed consent was waived. The deparaffinized sections were stained per standard IHC protocol. The antibodies used were AcAPE1 (1:200), Ki67 (1:500, CST, 9027), and SSRP1 (1:100). Staining intensity and percentage of positive cells were analyzed by Definiens Releases Tissue Studio 4.3. We used a stain deconvolution algorithm to separate the DAB chromogen stain and the hematoxylin counterstain in all tissue cores. We then measured the brown chromogen intensity across all tissues to obtain the range of pixel density. Based on the range, we divided the staining intensity into 3 categories using one-third threshold increment in the range. Tissue lysates were prepared and analyzed by Western blot as described previously (19).

Treatment response is assessed by the clinician using the modified Ryan Tumor Regression Grading System (20).
Complete response: No viable cancer cells
Moderate response: Single cells, or small groups of cancer cells
Minimal response: Residual cancer outgrown by fibrosis
No response: Minimal or no tumor killed; extensive residual cancer

Immunoprecipitation (IP) and FLAG-IP

Nuclear and chromatin extracts of HCT116 or RKO cells were precleared with protein A/G Plus agarose beads, and IP was performed with AcAPE1 antibody or control IgG (Santa Cruz, sc-2003). The chromatin extracts of control and MMS-treated cells were immunoprecipitated with the same antibody. FLAG-IP was done with mouse monoclonal α-FLAG M2 antibody–conjugated agarose beads (Sigma-Aldrich, A2220) in nuclear extracts of HEK293T cells transfected with FLAG-tagged constructs as described previously (18). The immunoprecipitated proteins were resolved in SDS-PAGE and identified by Western blot analysis with the indicated antibodies.

Immunofluorescence

Cells grown on coverslips were fixed with 4% formaldehyde (Sigma-Aldrich) and stained with immunofluorescence as described previously (16). Primary antibodies used were mouse monoclonal anti-APE1 (1:100; Novus Biologicals, NB100-116), anti-AcAPE1 (1:50), SSRP1 (1:100; BioLegend, 609702), and SPT16 (1:50; Abcam, 204343). Images were acquired by use of a fluorescence microscope with a 63 × oil immersion lens (LSM 510; Zeiss), and structured-illumination microscopy (SIM) was done with an Elyra PS.1 microscope (Carl Zeiss) by using a 63 × objective with a numerical aperture of 1.4. ImageJ software was used to measure Manders colocalization using the JaCoP plug-in.

Chromatin immunoprecipitation (ChIP) assay

ChIP assay was performed after double cross-linking of cells with disuccinimidyl glutarate and formaldehyde, with protein A/G Plus agarose beads (Santa Cruz, sc-2003) using with AcAPE1, SPT16, and control IgG (Santa Cruz) following the procedure as described earlier (16, 18). The immunoprecipitated purified DNA was used to amplify the p21 and DTL promoters regions using SYBR GREEN-based (Thermo Scientific) Real-Time PCR analysis. The following primers are used: p21 forward 5′-CAGGCTGTGGCTCTGATTGG-3′, reverse 5′-TTCAGAGTAACAGGCTAAGG-3′; DTL forward 5′-TCCTGCAAATTTCCCGCAAC-3′, reverse 5′-GGCTATGGCGAA-CAGGAACT-3′. Data were represented as relative enrichment with respect to IgG control based on the $2^{-\Delta CT}$ method.

AP site measurement assay

HCT116 cells were transfected with control and siRNA against SSRP1 and SPT16. After 48 hours, cells were treated with 1 mmol/L MMS for 1 hour and released in fresh media for 6 hours. Total genomic DNA was isolated by the Qiagen DNeasy kit following manufacturer's protocol. AP sites were measured using aldehyde reactive probe (Dojindo Laboratories) as described previously (16).

Fluorescence recovery after photobleaching

N-terminal GFP-tagged–APE1 (21) was transfected into HCT116 cells. Twenty-four hours after transfection of control and FACT siRNAs, cells were treated with DMSO or MMS. Fluorescence recovery after photobleaching (FRAP) experiments were performed as described previously (22). All FRAP data were normalized to the average prebleached fluorescence after removal of the background signal. The curve was plotted using GraphPad Prism 7, and each curve represented an average of 10 measurements from different regions of cells.

Xenograft studies

All animal experiments were performed following the approval of Institutional Animal Care and Use Committee. The experiments and reports are adhered to the Animal Research: Reporting of *In Vivo* Experiments (ARRIVE) guidelines. HCT116 and DLD-1 cells (2×10^6 in 100 μL medium) were injected subcutaneously over the left and right flanks in 6-week-old male athymic nude mice (Charles Rivers). The average weight was 27 ± 3.6 g. Subcutaneous tumors were allowed to grow for 1 to 2 weeks before treatments. The mice were divided into four treatment groups ($n = 5$ in each group) and received treatments every other day for 4 weeks. The drugs 5-FU 20 mg/kg, QC 50 mg/kg, and CBL0137 30 mg/kg were injected intraperitoneally. Combination group received both 5-FU and QC or CBL0137. Normal saline 100 μL was given to the control group. Body weight and tumors volume were measured before each treatment. The mice were euthanized in gas canister with gradual fill carbon dioxide after the end of treatment cycles. Xenograft tumor was fixed in formalin, and paraffin-embedded tissue sections were used to perform IHC staining Ki67 and TUNEL assay. The percentage of positive staining was quantified with 10 random high-power field images using TMARKER (23). Additive or synergistic effect was examined using online tool SynergyFinder (https://synergyfinder.fimm.fi; ref. 24).

Statistical analysis

Results are shown as the mean ± SEM of three independent experiments. Paired data were evaluated by Student *t* test, and one-way analysis of variance (ANOVA) was used for multiple comparisons. Friedman test was used for nonparametric test. A *P* value of less than 0.05 is considered statistically significant. *, $P < 0.05$; **, $P < 0.01$; ***, $P < 0.001$; ****, $P < 0.0001$.

Results

Downregulation of APE1 sensitizes dMMR colorectal cancer cells to 5-FU *in vitro*

To examine the role of APE1 in promoting 5-FU resistance in colorectal cancer, we used highly 5-FU resistant dMMR colon adenocarcinoma HCT116 (5) and isogenic HCT116 cells expressing APE1-specific shRNA (16). We found that downregulation of APE1 sensitized HCT116 to 5-FU (**Fig. 1A**). This phenomenon was confirmed in DLD-1 and HCT116 by siRNA interference (**Fig. 1B**), as evidenced by a decrease in the IC_{50} by approximately 10-fold (Supplementary Fig. S1).

APE1 interacts with nucleosome remodeling histone chaperone FACT complex in chromatin

In the absence of highly selective and nontoxic small-molecule inhibitors of DNA-repair function of APE1 (25), we set out to identify targets that regulate APE1 function in cells. To identify the interacting partners of AcAPE1, we immunoprecipitated (IP) endogenous AcAPE1 from the chromatin fraction using our AcAPE1-specific antibody. After separation in SDS-PAGE followed by the identification of protein bands by MALDI-TOF-TOF analysis, we identified a large number of proteins involved in the repair of damaged DNA as the prominent AcAPE1-interacting partners (**Fig. 1C**). We found DNA Ligase III, PARP1, both subunits (SPT16 and SSRP1) of the FACT complex, nucleolin, chromatin assembly factor 1a (CHAF1a), and all four core nucleosome histones H2A, H2B, H3, and H4 in the AcAPE1 IP complex. We focused on the FACT complex because increasing evidence suggests that the FACT complex plays a role at sites of UV damage and SSBs in cells (26, 27). The FACT complex, a heterodimer of structure-specific recognition protein 1 (SSRP1) and suppressor of Ty (SPT16), was originally identified as a histone chaperone complex that facilitates the removal and deposition of histone H2A/H2B in nucleosome during transcription initiation and elongation (28, 29). We confirmed the interaction of AcAPE1 with the FACT complex by immunoprecipitating AcAPE1 from nuclear and chromatin extracts followed by Western blot analysis. We found both subunits of FACT in AcAPE1 IPs, in both chromatin and nuclear fractions (**Fig. 1D** and **E**). Confocal microscopy revealed colocalization of AcAPE1 with SPT16 and SSRP1 in the nucleus (**Fig. 1F**). To examine whether acetylation of APE1 is required for its interaction with the FACT complex, we immunoprecipitated FLAG-tagged WT-APE1 and nonacetylable K5R mutant from nuclear fractions. No significant differences were observed in the amount of SPT16 bound with WT and nonacetylable K5R APE1 IPs, indicating that acetylation of APE1 is not essential for its interaction with the FACT complex (**Fig. 1G** and **H**). We also used the FLAG-tagged N-terminal 33 amino acids deleted NΔ33 mutant and K5Q APE1 mutant, which cannot enter the nucleus and stably bind to chromatin in cells (16, 21). Our data showed that inhibition of either nuclear localization or chromatin binding of APE1 significantly reduced the amount of SPT16 or SSRP1 in APE1 IP (**Fig. 1H**). Together, these data indicate that APE1 forms complex with FACT in chromatin, and acetylation is not essential for this interaction.

Induction of AP sites enhances colocalization of AcAPE1 and FACT in chromatin

To determine whether induction of DNA damage promotes interaction of APE1 and FACT at damage sites, we generated AP sites in the

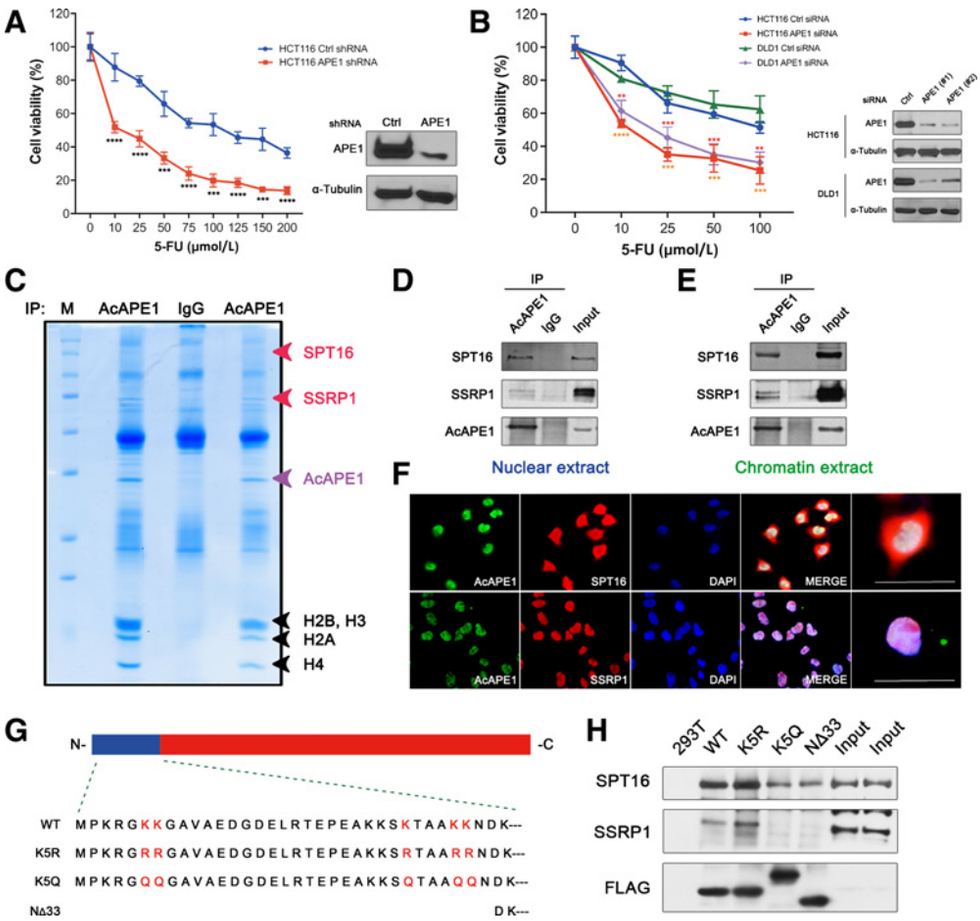

Figure 1.

APE1 plays a pivotal role in inducing 5-FU resistance in dMMR-CRC cells and interacts with SSRP1 and SPT16. **A,** HCT116 cells stably expressing control (ctrl) shRNA or APE1-shRNA were treated with various doses of 5-FU and viable cells were quantitated by MTT assay. APE1 levels in these cells were measured by immunoblot analysis. **B,** APE1 level in HCT116 and DLD-1 was downregulated by siRNA transfection, and cells were treated with 5-FU. Cell viability was measured by MTT. Immunoblot image showing the levels of APE1 after siRNAs transfection. Yellow asterisks mark the comparison between HCT116-ctrl siRNA and HCT116-APE1 siRNA. Red asterisks mark the comparison between DLD1-ctrl siRNA and DLD1-APE1 siRNA. **C,** Endogenous AcAPE1 in chromatin extracts was immunoprecipitated (IP) and resolved in SDS-PAGE gel followed by MALDI-TOF-TOF analysis. **D** and **E,** Co-IP followed by Western blot analysis showed the presence of SSRP1 and SPT16 in the AcAPE1 IP complex from nuclear and chromatin extracts. **F,** Colocalization of AcAPE1 with SPT16 and SSRP1 in nuclei was visualized using confocal microscope. Bar, 50 μm. **G,** Schematic diagram showing the mutation (red) and deletion sites in the N-terminus of APE1. **H,** Cells were transfected with FLAG-tagged WT-APE1 or mutant APE1 expression plasmids, and cell extracts were immunoprecipitated with FLAG antibody followed by Western blot analysis with SSRP1 and SPT16 antibodies.

genome by 5-FU or MMS treatment (a widely used alkylating agent that induces AP sites in the genome; ref. 30). SIM revealed enhanced colocalization of both subunits of the FACT complex with APE1 or AcAPE1 upon treatment (**Fig. 2A** and **B**; Supplementary Fig. S2). The Pearson correlation coefficient (PCC) was used to quantify the degree (+1 perfect correlation to −1 perfect but negative correlation) of colocalization between fluorophores (**Fig. 2C** and **D**). There was significant increase of colocalization of APE1 or AcAPE1 with the FACT complex upon induction of DNA damages, raising the possibility that recruitment of FACT to the damage sites may promote binding and acetylation of APE1 during the DNA-repair process. We examined the levels of FACT and AcAPE1 in chromatin fraction at several time points following MMS treatment. Treatment of MMS resulted in increasing levels of AcAPE1 and both subunits of the FACT complex in chromatin fraction in a time-dependent manner (**Fig. 2E**). Our Co-IP data showed that there was an increasing association of AcAPE1 and FACT complex upon induction of DNA damage (**Fig. 2F** and **G**). Previously, we showed that APE1 regulates p21 expression via binding to the *p21* and *DTL* proximal promoter regions and functions as a coactivator or corepressor depending on the p53 status of the cells (31). To understand if FACT facilitates the recruitment and/or binding of APE1 to damage sites in *p21* and *DTL* promoters, we treated the cells with MMS and cross-linked the chromatin. We performed ChIP assays with AcAPE1 and SPT16 antibodies. We found that induction of DNA damage significantly increased the binding/occupancy of AcAPE1 and SPT16 to the *p21* and *DTL* gene promoter regions (**Fig. 2H** and **I**).

FACT complex facilitates the binding and acetylation of APE1 to damage site in chromatin

To examine if FACT is required for facilitating the binding and acetylation of APE1 at damage sites in chromatin, we used siRNA to

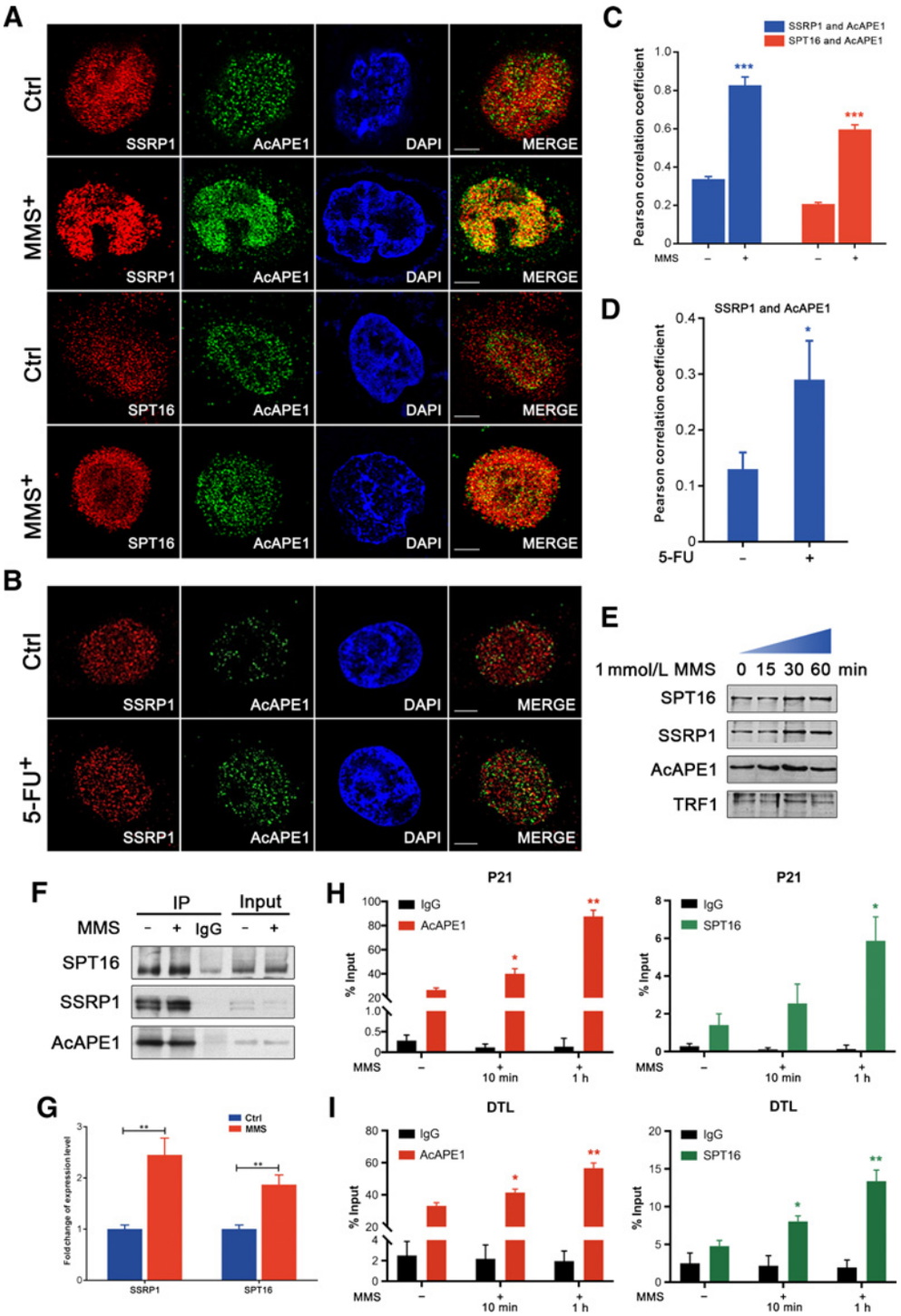

Figure 2.

Interaction of AcAPE1 with FACT complex enhances upon induction of DNA damages. **A** and **B,** Colocalization of SSRP1 or SPT16 with AcAPE1 in HCT116 cells before and after treatment with MMS or 5-FU was examined by SIM. Representative images are shown. Bar, 5 μm. **C** and **D,** PCC was used to quantify the colocalization of AcAPE1 with SSRP1 and SPT16. *, $P = 0.035$; ***, $P < 0.001$. **E,** Cells were treated with 1 mmol/L MMS for various time periods as indicated. AcAPE1, SSRP1, and SPT16 proteins levels were examined in chromatin extracts. **F,** AcAPE1 was immunoprecipitated after MMS treatment and immunoblotted with SSRP1 or SPT16 antibodies. **G,** Quantification of SPT16 and SSRP1 in IP from **F** showing the fold change of SSRP1 and SPT16 levels before and after MMS treatment. **H** and **I,** Occupancy of AcAPE1 and SPT16 to *p21* and *DTL* promoter regions was examined before and after treatment with MMS by ChIP analysis.

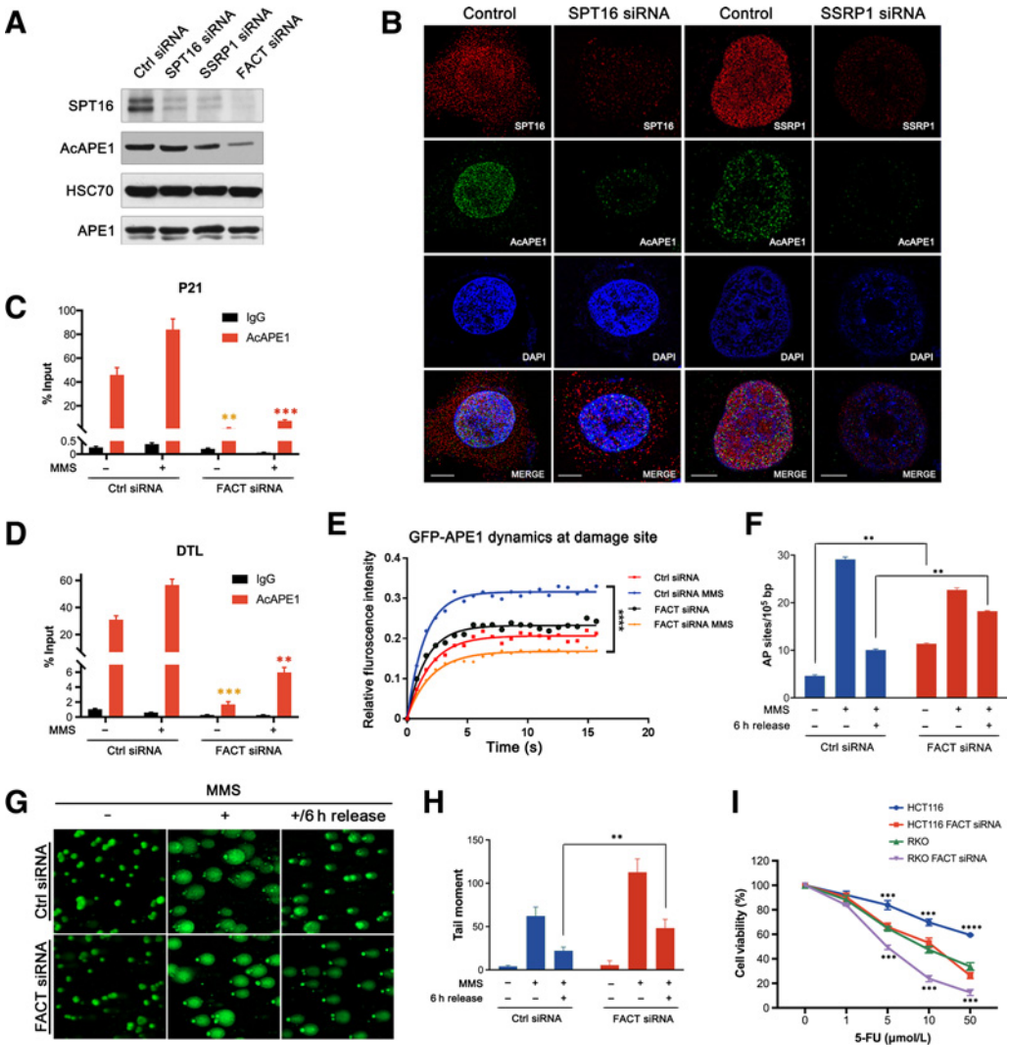

Figure 3.

FACT complex facilitates AP site and SSB repair by facilitating APE1 access and acetylation in chromatin. **A,** SPT16 or SSRP1 level individually or both together (FACT) was downregulated by siRNA for 24 hours and the levels of AcAPE1 and APE1 were measured by immunoblot analysis. Note that FACT siRNA means siRNAs of SSRP1 plus SPT16. **B,** AcAPE1 level was examined in SPT16 and SSRP1 downregulated cells by SIM. **C** and **D,** Occupancy of AcAPE1 to *p21* and *DTL* promoters was examined before and after treatment with MMS by ChIP analysis. Yellow asterisks mark the comparisons between ctrl siRNA and FACT siRNA without MMS treatment. Red asterisks mark the comparisons between ctrl siRNA and FACT siRNA at the presence of MMS. **E,** GFP-tagged APE1 expression plasmid was transfected in control or FACT downregulated cells and specific regions were bleached with laser and the recovery of GFP fluorescence was examined. **F,** Control and FACT downregulated cells were treated with MMS and then release for 6 hours. The number of AP sites in the genomic DNA was quantitated using aldehyde reactive probe. **G,** Control and FACT downregulated cells were treated with MMS and release for 6 hours. DNA damage was examined by single-cell alkaline comet assay. **H,** Average tail moment before and after MMS treatment was shown. **I,** Cell viability were examined after FACT KD in HCT116 and RKO cells.

downregulate SPT16 and SSRP1 individually and both together (**Fig. 3A**). Consistent with a prior report, we found that downregulation of either subunit SPT16 or SSRP1 affected the level of the other subunit in cells (32). We found a significant decrease of the AcAPE1 level when both subunits of FACT were downregulated (**Fig. 3A**). SIM demonstrated that FACT knockdown reduced the AcAPE1 level but did not alter the total APE1 level in cells (**Fig. 3B** and Supplementary Fig. S3A). As acetylation of APE1 occurs after binding to the AP site in chromatin, these data indicate that the absence of the FACT complex significantly reduced the access or binding of APE1 to damage sites and its subsequent acetylation in chromatin. We examined the binding or occupancy of unmodified APE1 and AcAPE1 to *p21* and *DTL* promoter in FACT downregulated cells by ChIP assays. ChIP assays revealed that FACT downregulation significantly abrogated the occupancy of APE1 and AcAPE1 to *p21* and *DTL* promoters upon DNA damages (**Fig. 3C** and **D** and Supplementary Fig. S3B–S3C). Together, these data provide evidence that the FACT complex promotes the binding and subsequent acetylation of APE1 to damage sites in chromatin.

To further examine the role of FACT in regulating APE1 binding dynamics to damage sites, we used FRAP (33) to quantify the mobility of GFP-tagged APE1 in the presence or absence of the FACT complex. Fluorescence was bleached using an excitation laser, and the recovery of fluorescence in that region due to binding of new GFP-tagged APE1

into chromatin was monitored (33). The mobile fraction represents the fraction of recovered fluorescence and the half-life ($T_{1/2}$) is the time it takes for fluorescence intensity to reach half the maximum of the plateau level. In the presence of MMS, the mobile fraction of APE1 in FACT downregulated cells was significantly lower compared with control cells (**Fig. 3E**), suggesting that FACT regulates the mobility and binding dynamics of APE1 to damage sites in chromatin.

FACT is required for efficient repair of AP site damages in cells, and downregulation of FACT sensitizes colorectal cancer cells to 5-FU

As FACT promotes binding and subsequent acetylation of APE1, we deduced that cells would accumulate AP sites in the absence of FACT. We depleted the FACT complex by siRNA and quantitated AP sites in the genome. As expected, depleting the FACT complex significantly increased the number of AP sites in the genome compared with control (**Fig. 3F**). We also treated these cells with MMS to induce AP site damages. As shown in **Fig. 3F**, AP sites accumulated significantly in the genome after MMS treatment in both control and FACT downregulated cells. However, after 6 hours of release, FACT knockdown cells retained significantly more AP sites, indicating that efficient AP site repair depends on the function of the FACT complex. To provide further evidence for the role of FACT in facilitating the AP site or SSBs repair in cells, we used single-cell alkaline comet assay that detects the SSB and DSB damages in the genome in cells. Knockdown of FACT significantly delayed the repair of MMS-induced DNA damages in the genome compared with control cells (**Fig. 3G** and **H**). Consistently, we found that downregulation of FACT sensitizes HCT116 and RKO cell lines to 5-FU (**Fig. 3I**). Together, these data indicate that FACT complex plays a crucial role in the AP site or SSBs repair in cells.

Targeting FACT with curaxins enhances the efficacy of 5-FU in dMMR colorectal cancer cells *in vitro*

Several studies have shown that curaxins, a class of small-molecule drugs (Supplementary Fig. S4A), have broad anticancer activity and function as an inhibitor of the FACT complex (34–36). FACT binds to unfolded nucleosomes and curaxins trap FACT in chromatin (34). Consistent with previous studies, our data show that QC (37), a first-generation curaxin, reduced SSRP1 and SPT16 levels from soluble nuclear fraction but had no effect on the chromatin-bound fraction (**Fig. 4A**). CBL0137, a second-generation curaxin (38), exhibited a similar effect on the FACT complex and decreased the level of AcAPE1, while the total APE1 level remained unchanged (**Fig. 4B–D** and Supplementary Fig. S4B). Of note, we found that HCT116 cells were unable to repair 5-FU- or MMS-induced damage in the presence of the FACT inhibitor CBL0137 (**Fig. 4E** and **F**; Supplementary Fig. S4C–S4D). Because our studies and others show that FACT is involved in the AP site or SSBs repair in cells, we examined whether targeting FACT with CBL0137 enhanced the efficacy of 5-FU in dMMR colorectal cancer *in vitro*. To eliminate the possibility that QC or CBL0137 shows a cytotoxic effect per se by inducing DNA damages, cells were treated with different doses of QC or CBL0137 alone. We found minimal DNA damage with treatment of increasing doses of CBL0137 treatment on the comet assay (Supplementary Fig. S4E). Moreover, 4 μmol/L CBL0137 or 10 μmol/L QC alone had a minimal effect (20% cell death) on cell viability (Supplementary Fig. S4F and S4G). However, combination of 2 μmol/L CBL0137 or 5 μmol/L QC with 5-FU significantly enhanced the sensitivity (∼50-fold decrease in IC_{50}) of 5-FU–resistant dMMR HCT116 and RKO cells to 5-FU (**Fig. 4G** and **H**), suggesting that targeting the FACT complex with curaxins could be a promising strategy to overcome 5-FU resistance in dMMR colorectal cancer cells *in vivo*.

FACT inhibitor curaxin sensitizes dMMR colorectal cancer tumor to 5-FU *in vivo*

To examine whether the combination of curaxins and 5-FU inhibits dMMR colorectal cancer tumor growth *in vivo*, we utilized tumor xenograft models. The effects of QC and CBL0137 were tested alone and in combination of 5-FU. The tumor growth curve showed that single-agent treatment with 5-FU, QC, or CBL0137 alone had very little or moderate effect on tumor growth compared with the vehicle group (**Fig. 5A–D**; Supplementary Fig. S5A–S5D), while the combination group significantly inhibited tumor growth, demonstrating a synergistic effect. The combination of QC with 5-FU was well tolerated at the scheduled doses. All mice were weighted at each time point of treatment during the study, and there was 10% to 15% total weight loss at the end of the study period. No cachectic appearance was noted (Supplementary Fig. S5E). Moreover, no major histologic abnormality was identified in vital organs, including lung, liver, and kidney (Supplementary Fig. S5F). Further analysis showed that the combination group suppressed the proliferation and induced apoptosis in these tumors (**Fig. 5E–H**). Additionally, long-term QC treatment resulted in decreased SSRP1 level in the nucleus, and the residual SSRP1 was trapped in chromatin (**Fig. 5I**), suggesting that QC alters FACT expression and localization *in vivo*. These data together demonstrate that inhibition of FACT function with curaxins can overcome 5-FU resistance and inhibits dMMR colorectal cancer growth both *in vitro* and *in vivo*.

FACT is overexpressed in colon cancer tissue and cell lines

Previously, we showed that primary tumor tissues of colorectal cancer and other types of cancer patients have higher AcAPE1 levels compared with adjacent-nontumor tissues (19, 39). Recent reports demonstrate that FACT expression is strongly associated with poorly differentiated cancers and low overall survival (32, 35, 36, 38). Here, we examined the levels of SSRP1 and AcAPE1 in colorectal cancer patients' tumor tissues. Both subunits of the FACT complex and AcAPE1 were overexpressed in tumor but not in adjacent normal tissues (**Fig. 6A** and **B**). This finding was confirmed in various colon cancer cell lines using HCEC cells for comparison (**Fig. 6C** and **D**). These data indicate a potential role of overexpression of FACT and AcAPE1 in inducing chemoresistance.

FACT (SSRP1) expression and AcAPE1 levels positively correlate with chemoresistance in colorectal cancer patients

To determine the clinical significance of elevated levels of FACT and AcAPE1 in colorectal cancer, we extended our analyses by assessing SSRP1 and AcAPE1 levels in 39 colorectal cancer patients at different T stages. Among them, 19 patients had a moderate response and the other 20 had no response or minimal response to chemotherapy. Four (10.3%) were characterized as microsatellite instable or MMR deficient. This is consistent with prior reports that sporadic, noninherited dMMR colorectal cancer constitutes 10% to 15% of all colorectal cancers (40). The percentages of positive cells and the staining intensity of SSRP1 and AcAPE1 level were significantly higher in colorectal cancer tumor tissue compared with control (**Fig. 6E**). Although SSRP1 or AcAPE1 staining varied among the samples within a particular stage of colorectal cancer, we found a significant increase in the percentage of positive SSRP1 and AcAPE1 staining cells from stage T2 to T4,

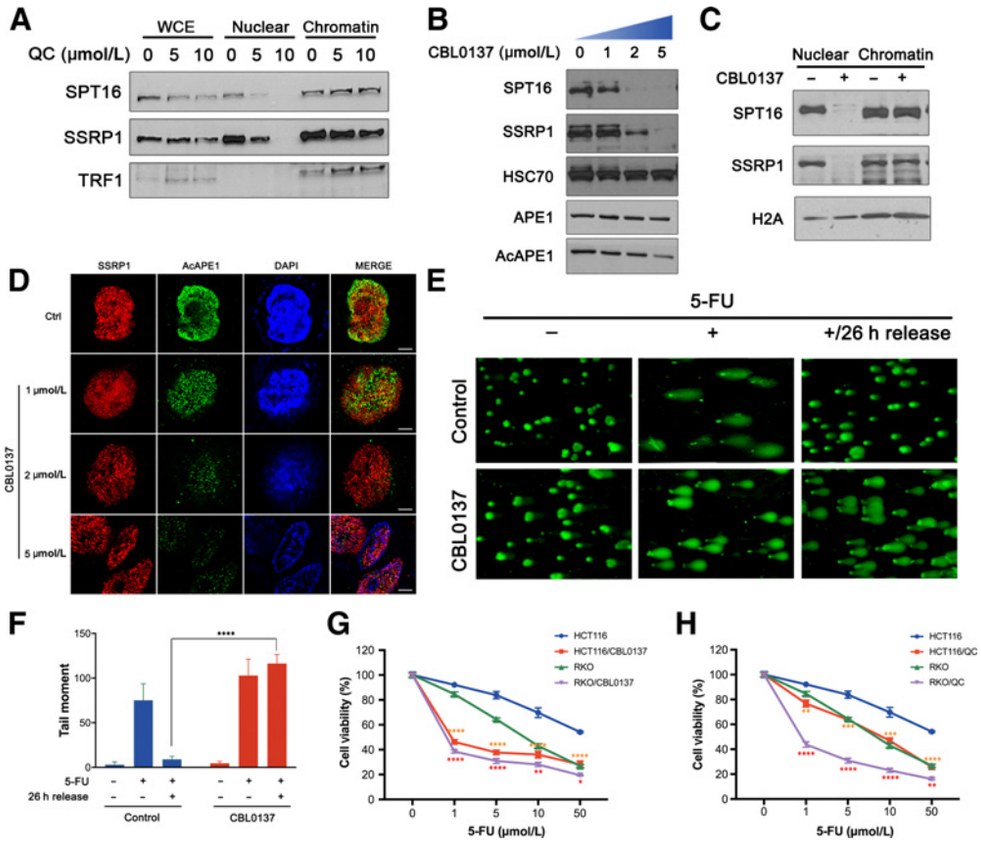

Figure 4.

FACT inhibitor curaxin inhibits efficient repair of 5-FU induced DNA damages and sensitizes dMMR colorectal cancer cells to 5-FU *in vitro*. **A–C,** HCT116 cells were treated with indicated doses of QC or CBL0137 for 1 hour, and whole-cell extract (WCE), soluble nuclear, and chromatin-bound fractions were prepared. SSRP1 and SPT16 levels in these extracts were examined by immunoblot analysis. **D,** Cells were treated with indicated doses of CBL0137 for 1 hour, and the AcAPE1 level in cells was examined by SIM. **E,** HCT116 cells, pretreated with or without CBL0137 for 1 hour, were exposed to 5-FU for 6 hours and then allowed to recover for 26 hours. DNA damage was examined by alkaline comet assay. **F,** Average tail moment before and after 5-FU treatment was shown. **G** and **H,** HCT116 and RKO were treated with and without QC or CBL0137 for 1 hour then exposed to various doses of 5-FU. Cell viability was measured by MTT assay. Yellow asterisks mark the comparisons between HCT116 and HCT116/CBL0137 (**G**) or HCT116 and HCT116/QC (**H**). Red asterisks mark the comparisons between RKO and RKO/CBL0137 (**G**) or RKO and RKO/QC (**H**).

indicating that SSRP1 and AcAPE1 level increases with tumor depth invasion (**Fig. 6F** and **G**). Analysis of staining intensity of AcAPE1 and SSRP1 in tumor samples (characterized as low, medium, and high intensity) revealed higher numbers of positive cells, exhibiting high intensity staining with increasing tumor stage (**Fig. 6H** and **I**).

Next, we determined the relationship between FACT expression and acetylation of APE1 across all patient samples. We revealed a moderate but significantly positive correlation between SSRP1 and AcAPE1 levels in colorectal cancer samples (**Fig. 7A**). We found that patients exhibiting no or minimal response to 5-FU had distinct staining patterns compared with patients exhibiting moderate responses (**Fig. 7B**). Quantitation of the percentage of positive staining cells showed that the percentage of positive SSRP1 or AcAPE1 was 2-fold higher in nonresponders or minimal responders compared with moderate responders (**Fig. 7C** and **D**). Additionally, three out of four patients who have loss of MSH2 and MSH6 were found to have minimal or no response, and they had high levels of AcAPE1 and FACT (Supplementary Fig. S6). Overall, these data indicate that the expression levels of SSRP1 and AcAPE1 positively correlate with 5-FU resistance in colorectal cancer patients.

Discussion

Resistance to 5-FU remains a major challenge in the treatment of dMMR colorectal cancer. Several mechanisms are believed to contribute to 5-FU resistance, including overexpression of TS enzyme due to gene amplification, deficient MMR pathway activity, and enhanced DNA damage repair resulting in reduced apoptosis (2, 41). However, TS levels do not explain the observed therapeutic resistance to 5-FU in dMMR colorectal cancer (42), and several clinical studies have shown that defective mismatch repair is a strong predictor for the lack of response of 5-FU–based adjuvant therapy in dMMR colorectal cancer (2). Here, we demonstrate that loss of APE1 significantly sensitizes dMMR colorectal cancer to 5-FU, indicating the significant role of the BER pathway in dMMR colorectal cancer.

Overexpression of APE1 in different cancer types, including colorectal cancer, and its association with chemotherapeutic resistance as well as poor prognosis are well documented (43). AP sites or SSB are common intermediates in the BER pathway that are generated after the removal of damages bases induced by many chemotherapeutic drugs, including 5-FU and alkylating agents (13).

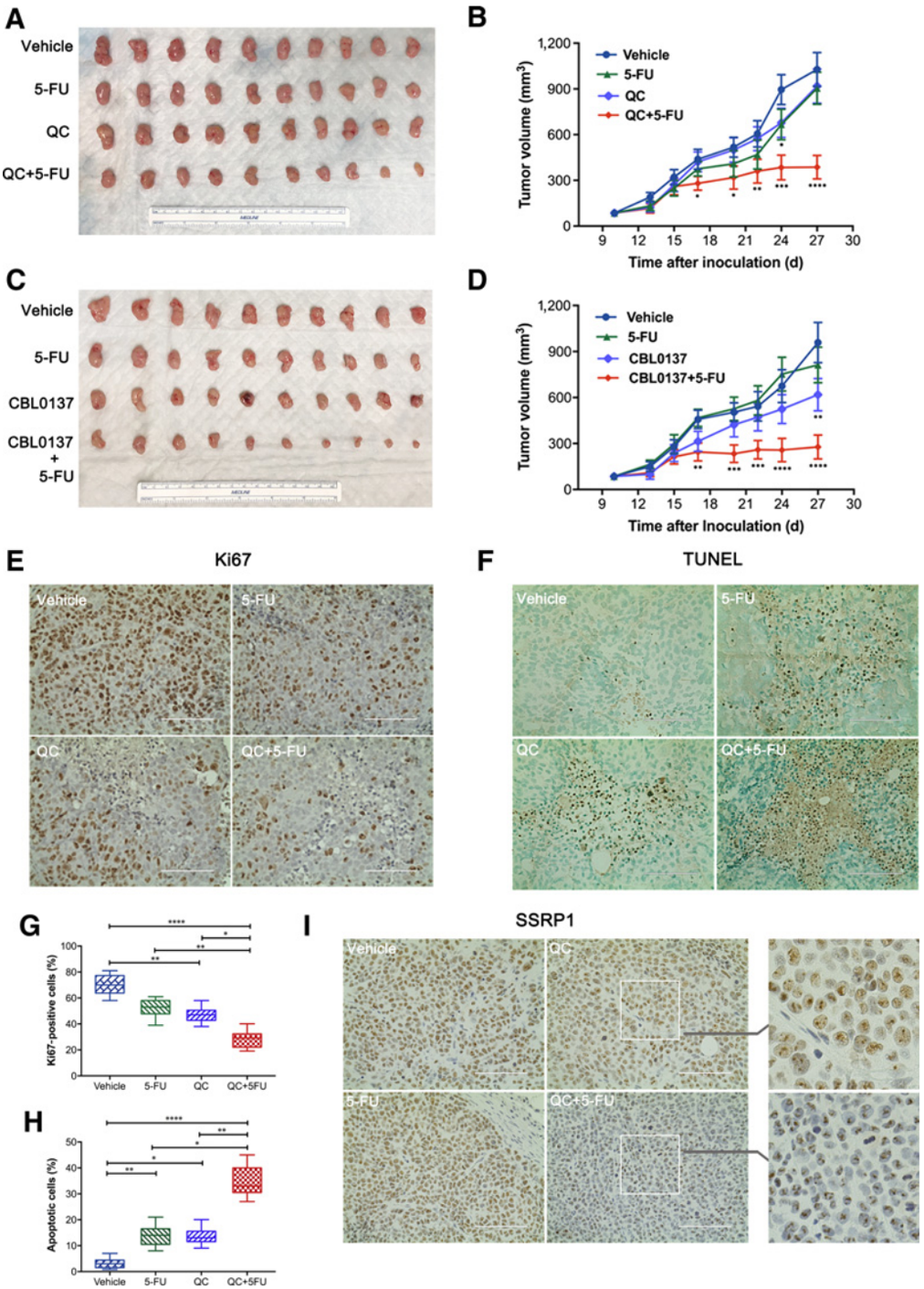

Figure 5.

FACT inhibitor curaxin sensitizes dMMR colorectal cancer tumor growth *in vivo*. **A** and **C,** Vehicle, 5-FU, QC, and combination of 5-FU and QC were administered to mice intraperitoneally for 3 weeks (**A**). In a separate experiment, 5-FU, CBL0137, and combination of 5-FU and CBL0137 were used (**C**). Resected xenograft tumors after completion of treatment are shown. **B** and **D,** Tumor volume was measured at indicated days, and tumor growth curve was plotted. **E,** Paraformaldehyde-fixed xenograft tumor section from each treatment groups was stained for Ki67 to examine cell proliferation. **F,** TUNEL assay was performed in tumor sections and the representative images are shown. **G** and **H,** Box chart depicting the Ki67 or TUNEL-positive cell percentage among groups. Data report the median, 25th and 75th percentiles of percentages of positive cells. **I,** Tumor sections from each treatment groups were stained with SSRP1 antibody. Zoomed images of portions of the IHC staining indicate the chromatin trapping of FACT due to QC treatment.

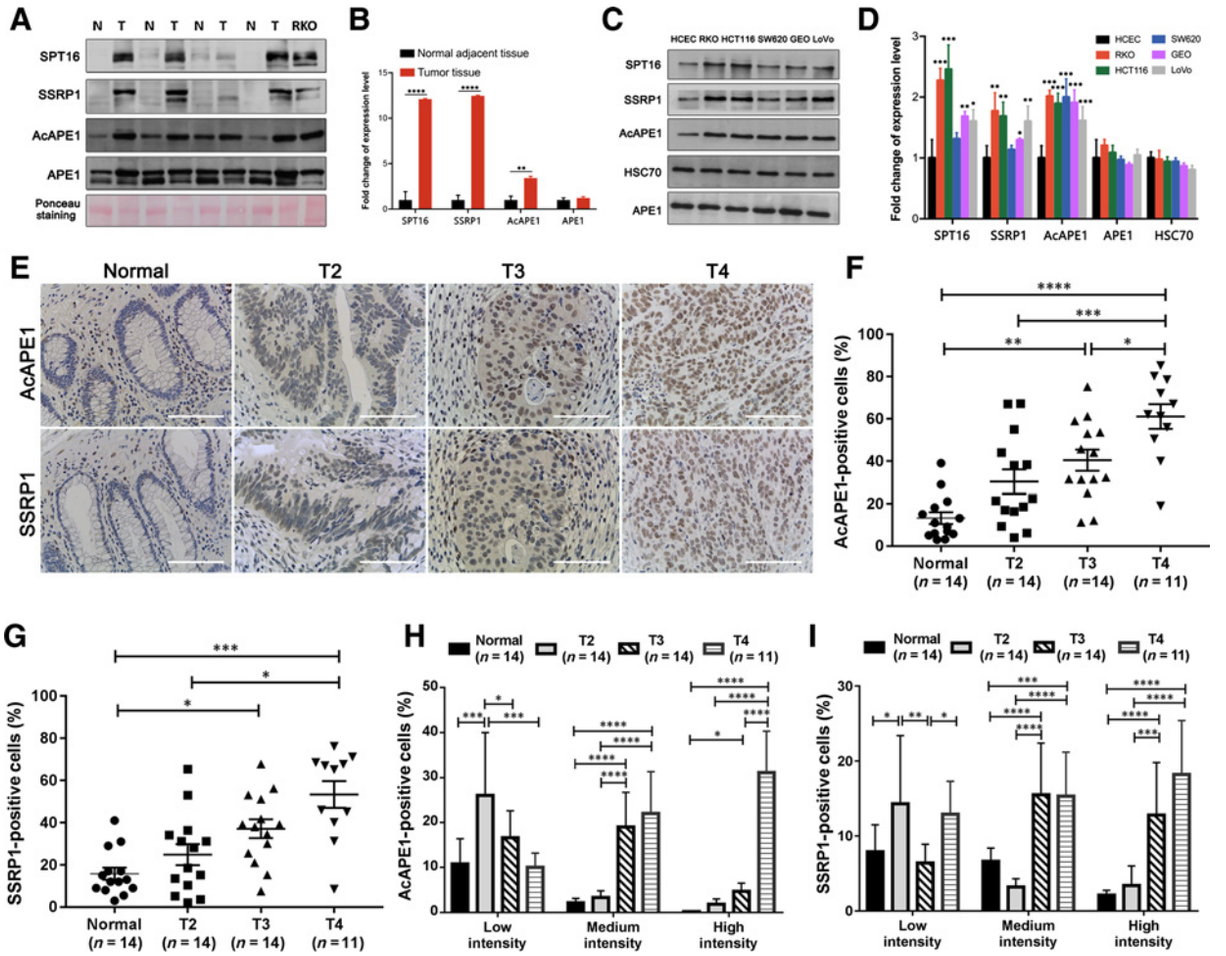

Figure 6.

AcAPE1 and SSRP1 levels are elevated in human colorectal cancer samples and colorectal cancer cell lines. **A,** Levels of APE1, AcAPE1, SSRP1, and SPT16 in paired adjacent normal (N) and tumor (T) tissue extracts of colorectal cancer patients. **B,** The expression level of each protein in tumors was presented in fold change compared with normal adjacent tissues. Data were expressed as mean ± SEM of three independent experiments. **C,** The levels of AcAPE1, SSRP1, and SPT16 were analyzed in various colon cancer cell lines as compared with the normal colon cell line HCEC. **D,** Bar graph showing elevated levels of SPT16, SSRP1, and AcAPE1 in multiple colorectal cancer cell lines compared with normal HCEC cells. Expression levels were presented in fold change with respect to normal HCEC cells. **E,** IHC staining of AcAPE1 and SSRP1 from a total of 39 colorectal cancer patients with different T stages was performed. Representative images are shown. **F** and **G,** The percentage of cells positive for AcAPE1 or SSRP1 from 10 random high field in each sample was pooled. **H** and **I,** The percentage of cells with low, medium, and high staining intensity in each group was analyzed and plotted.

The repair of AP sites/SSBs by APE1 on naked DNA or nucleosomal DNA substrate has been extensively investigated *in vitro* (44). However, to date, how APE1 repairs AP sites in the context of the nucleosome in chromatin remains largely unknown. Earlier, we discovered that human APE1 could be acetylated (AcAPE1) at multiple lysine (Lys 6, 7, 27, 31, 32, and 35) residues in the N-terminal domain by p300 (16, 45). Acetylation of these Lys residues modulates both DNA damage repair function of APE1 and the expression of multiple genes (16, 18, 45). Furthermore, we demonstrated that tumor tissues of diverse origins have higher levels of acetylated APE1 and the absence of APE1 acetylation sensitizes cells to many chemotherapeutic agents (19). It is likely that at the initiating steps of repair, DNA glycosylase responsible for removing the incorporated 5-FU facilitates the recruitment of FACT to sites of damage through physical interaction. Consistent with this, SSRP1 was shown to interact with OGG1 DNA glycosylase (46). We predict that FACT remains at damage sites and might cooperate to facilitate complete repair by promoting chromatin relaxation and subsequent recruitment of downstream repair proteins APE1 and XRCC1 through physical interaction (27). This may also facilitate the recruitment of histone acetyltransferase p300 to acetylate APE1 and acetylation in turn enhances the endonuclease activity of APE1 and promotes faster repair. Consistent with this hypothesis, a recent study shows that SSRP1 cooperates with PARP1 and XRCC1 to facilitate SSBs repair by chromatin priming (27).

The second-generation curaxin CBL0137 is in the phase I multicenter clinical trial for metastatic or unresectable advanced solid malignancies (NCT01905228). This small-molecule modulates several important signaling pathways through inhibition of FACT function (35, 36). Increasing evidence suggests that CBL0137 itself has low direct cytotoxic effects (34, 38). Our data also suggest that combination of curaxins with 5-FU has no major toxicity in vital

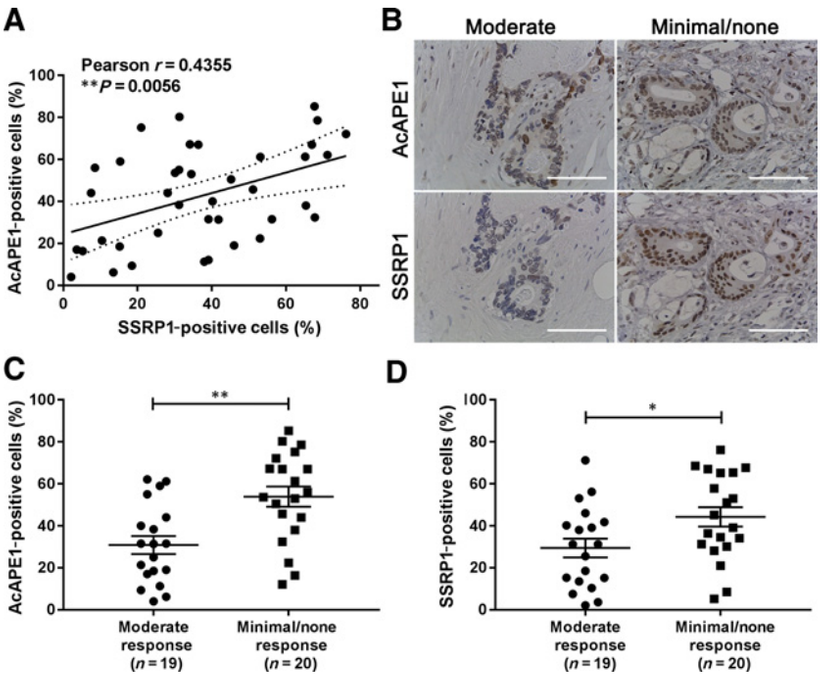

Figure 7.
Elevated level of AcAPE1 or SSRP1 in colorectal cancer patients is associated with poor treatment response to chemotherapy. **A,** The expression of AcAPE1 and SSRP1 was analyzed using linear regression. **B,** Representative images of AcAPE1 and SSRP1 staining in patients with moderate and minimal/none response to chemotherapy are shown. **C** and **D,** The percentages of cells with positive AcAPE1 and SSRP1 staining were compared between moderate and minimal/none response groups.

organs in mice. Studies have shown that curaxins do not cause DNA damage or affect general transcription and are therefore expected to be well tolerated (35). We propose that combination of CBL0137 has several advantages, including high efficiency in reaching nuclear DNA (as they are not substrate for multidrug transporters) and high DNA affinity that facilitates altering nucleosome without causing DNA damage (34). Although our data show that combination of CBL0137 with 5-FU inhibits DNA damage repair and provides better cell killing *in vivo*, we cannot eliminate the possibility that curaxins also affect the expression of other genes involved in modulating the tumor growth or sensitivity to 5-FU.

In conclusion, our study identifies the FACT complex as the interacting partner of APE1 and discovers a novel role of FACT in inducing 5-FU resistance via modulating the APE1-dependent BER pathway. The FACT complex facilitates the recruitment and acetylation of APE1, which in turn promotes 5-FU resistance in dMMR colorectal cancer. In this preclinical study, we have shown that targeting the FACT complex with small molecules CBL0137/curaxin significantly improves the efficacy of 5-FU in dMMR colorectal cancer *in vitro* and *in vivo*. The readily available small-molecule CBL0137 warrants further testing to determine its biodistribution, efficacy, and toxicity profile *in vivo*. The combination therapy represents a highly translatable and targeted therapeutic approach that can be used clinically to overcome 5-FU resistance in dMMR colorectal cancer patients after further validation.

Disclosure of Potential Conflicts of Interest

No potential conflicts of interest were disclosed.

Authors' Contributions

Conception and design: H. Song, V. Band, K.K. Bhakat
Development of methodology: H. Song, J. Zeng, B. Mohapatra
Acquisition of data (provided animals, acquired and managed patients, provided facilities, etc.): H. Song, J. Zeng, S. Roychoudhury, P. Biswas, K. Dowlatshahi
Analysis and interpretation of data (e.g., statistical analysis, biostatistics, computational analysis): H. Song, J. Zeng, S. Ray, K. Dowlatshahi, J. Wang, G. Talmon, K.K. Bhakat
Writing, review, and/or revision of the manuscript: H. Song, J. Zeng, B. Mohapatra, J. Wang, G. Talmon, K.K. Bhakat
Study supervision: K.K. Bhakat

Acknowledgments

We would like to thank Dan Feng for her technical assistance. We sincerely thank Dr. Michael Hollingsworth for his critical reading of the manuscript. We appreciate Lijun Sun and Jiang Jiang from UNMC Tissue Sciences Facility for assisting with tissue sections and histochemical staining. We are very thankful to Incuron Inc. and Dr. Andrei A. Purmal for providing CBL0137 for our study. We thank Janice A. Taylor and James R. Talaska of the Advanced Microscopy Core Facility at the University of Nebraska Medical Center for providing assistance with (confocal and super resolution) microscopy. This work was supported by NIH/NCI funding R01CA148941 and Nebraska Department of Health and Human Services LB-506 to K. Bhakat. H. Song is supported by UNMC graduate assistant fellowship. The UNMC Advanced Confocal Microscopy Lab is funded by the Nebraska Research Initiative and Fred and Pamela Buffet Cancer Center support grant P30 CA036727.

The costs of publication of this article were defrayed in part by the payment of page charges. This article must therefore be hereby marked *advertisement* in accordance with 18 U.S.C. Section 1734 solely to indicate this fact.

Received June 13, 2019; revised August 20, 2019; accepted September 24, 2019; published first October 1, 2019.

References

1. Andre T, Boni C, Mounedji-Boudiaf L, Navarro M, Tabernero J, Hickish T, et al. Oxaliplatin, fluorouracil, and leucovorin as adjuvant treatment for colon cancer. N Engl J Med 2004;350:2343–51.
2. Ribic CM, Sargent DJ, Moore MJ, Thibodeau SN, French AJ, Goldberg RM, et al. Tumor microsatellite-instability status as a predictor of benefit from fluorouracil-based adjuvant chemotherapy for colon cancer. N Engl J Med 2003;349:247–57.

3. Carethers JM, Smith EJ, Behling CA, Nguyen L, Tajima A, Doctolero RT, et al. Use of 5-fluorouracil and survival in patients with microsatellite-unstable colorectal cancer. Gastroenterology 2004;126:394–401.
4. Sinicrope FA, Mahoney MR, Smyrk TC, Thibodeau SN, Warren RS, Bertagnolli MM, et al. Prognostic impact of deficient DNA mismatch repair in patients with stage III colon cancer from a randomized trial of FOLFOX-based adjuvant chemotherapy. J Clin Oncol 2013;31:3664–72.
5. Bracht K, Nicholls AM, Liu Y, Bodmer WF. 5-Fluorouracil response in a large panel of colorectal cancer cell lines is associated with mismatch repair deficiency. Br J Cancer 2010;103:340–6.
6. Longley DB, Harkin DP, Johnston PG. 5-fluorouracil: mechanisms of action and clinical strategies. Nat Rev Cancer 2003;3:330–8.
7. Sawyer RC, Stolfi RL, Martin DS, Spiegelman S. Incorporation of 5-fluorouracil into murine bone marrow DNA in vivo. Cancer Res 1984;44:1847–51.
8. Kunz C, Focke F, Saito Y, Schuermann D, Lettieri T, Selfridge J, et al. Base excision by thymine DNA glycosylase mediates DNA-directed cytotoxicity of 5-fluorouracil. PLoS Biol 2009;7:e91.
9. Fischer F, Baerenfaller K, Jiricny J. 5-Fluorouracil is efficiently removed from DNA by the base excision and mismatch repair systems. Gastroenterology 2007; 133:1858–68.
10. Tajima A, Hess MT, Cabrera BL, Kolodner RD, Carethers JM. The mismatch repair complex hMutS alpha recognizes 5-fluorouracil-modified DNA: implications for chemosensitivity and resistance. Gastroenterology 2004;127:1678–84.
11. Meyers M, Wagner MW, Hwang H-S, Kinsella TJ, Boothman DA. Role of the hMLH1 DNA mismatch repair protein in fluoropyrimidine-mediated cell death and cell cycle responses. Cancer Res 2001;61:5193.
12. Mauro DJ, De Riel JK, Tallarida RJ, Sirover MA. Mechanisms of excision of 5-fluorouracil by uracil DNA glycosylase in normal human cells. Mol Pharmacol 1993;43:854–7.
13. Li M, Wilson DM 3rd. Human apurinic/apyrimidinic endonuclease 1. Antioxid Redox Signal 2014;20:678–707.
14. Chattopadhyay R, Das S, Maiti AK, Boldogh I, Xie J, Hazra TK, et al. Regulatory role of human AP-endonuclease (APE1/Ref-1) in YB-1-mediated activation of the multidrug resistance gene MDR1. Mol Cell Biol 2008;28:7066–80.
15. Mitra S, Izumi T, Boldogh I, Bhakat KK, Hill JW, Hazra TK. Choreography of oxidative damage repair in mammalian genomes. Free Radic Biol Med 2002;33: 15–28.
16. Roychoudhury S, Nath S, Song H, Hegde ML, Bellot LJ, Mantha AK, et al. Human apurinic/apyrimidinic endonuclease (APE1) is acetylated at DNA damage sites in chromatin, and acetylation modulates its DNA repair activity. Mol Cell Biol 2017;37. doi: 10.1128/MCB.00401-16.
17. Nath S, Roychoudhury S, Kling MJ, Song H, Biswas P, Shukla A, et al. The extracellular role of DNA damage repair protein APE1 in regulation of IL-6 expression. Cell Signal 2017;39:18–31.
18. Sengupta S, Mantha AK, Mitra S, Bhakat KK. Human AP endonuclease (APE1/ Ref-1) and its acetylation regulate YB-1-p300 recruitment and RNA polymerase II loading in the drug-induced activation of multidrug resistance gene MDR1. Oncogene 2011;30:482–93.
19. Sengupta S, Mantha AK, Song H, Roychoudhury S, Nath S, Ray S, et al. Elevated level of acetylation of APE1 in tumor cells modulates DNA damage repair. Oncotarget 2016;7:75197–209.
20. Kim SH, Chang HJ, Kim DY, Park JW, Baek JY, Kim SY, et al. What is the ideal tumor regression grading system in rectal cancer patients after preoperative chemoradiotherapy? Cancer Res Treat 2016;48:998–1009.
21. Jackson EB, Theriot CA, Chattopadhyay R, Mitra S, Izumi T. Analysis of nuclear transport signals in the human apurinic/apyrimidinic endonuclease (APE1/ Ref1). Nucleic Acids Res 2005;33:3303–12.
22. Hoogstraten D, Nigg AL, Heath H, Mullenders LH, van Driel R, Hoeijmakers JH, et al. Rapid switching of TFIIH between RNA polymerase I and II transcription and DNA repair in vivo. Mol Cell 2002;10:1163–74.
23. Schuffler PJ, Fuchs TJ, Ong CS, Wild PJ, Rupp NJ, Buhmann JM. TMARKER: A free software toolkit for histopathological cell counting and staining estimation. J Pathol Inform 2013;4(Suppl):S2.
24. Ianevski A, He L, Aittokallio T, Tang J. SynergyFinder: a web application for analyzing drug combination dose-response matrix data. Bioinformatics 2017;33: 2413–5.
25. Gordon MS, Rosen LS, Mendelson D, Ramanathan RK, Goldman J, Liu L, et al. A phase 1 study of TRC102, an inhibitor of base excision repair, and pemetrexed in patients with advanced solid tumors. Invest New Drugs 2013;31:714–23.
26. Dinant C, Ampatziadis-Michailidis G, Lans H, Tresini M, Lagarou A, Grosbart M, et al. Enhanced chromatin dynamics by FACT promotes transcriptional restart after UV-induced DNA damage. Mol Cell 2013;51:469–79.
27. Gao Y, Li C, Wei L, Teng Y, Nakajima S, Chen X, et al. SSRP1 cooperates with PARP and XRCC1 to facilitate single-strand DNA break repair by chromatin priming. Cancer Res 2017;77:2674–85.
28. Belotserkovskaya R, Oh S, Bondarenko VA, Orphanides G, Studitsky VM, Reinberg D. FACT facilitates transcription-dependent nucleosome alteration. Science 2003;301:1090–3.
29. Winkler DD, Luger K. The histone chaperone FACT: structural insights and mechanisms for nucleosome reorganization. J Biol Chem 2011;286:18369–74.
30. Wyatt MD, Pittman DL. Methylating agents and DNA repair responses: methylated bases and sources of strand breaks. Chem Res Toxicol 2006;19: 1580–94.
31. Sengupta S, Mitra S, Bhakat KK. Dual regulatory roles of human AP-endonuclease (APE1/Ref-1) in CDKN1A/p21 expression. PLoS One 2013;8: e68467.
32. Garcia H, Miecznikowski JC, Safina A, Commane M, Ruusulehto A, Kilpinen S, et al. Facilitates chromatin transcription complex is an "accelerator" of tumor transformation and potential marker and target of aggressive cancers. Cell Rep 2013;4:159–73.
33. Reits EA, Neefjes JJ. From fixed to FRAP: measuring protein mobility and activity in living cells. Nat Cell Biol 2001;3:E145–7.
34. Nesher E, Safina A, Aljahdali I, Portwood S, Wang ES, Koman I, et al. Role of chromatin damage and chromatin trapping of FACT in mediating the anticancer cytotoxicity of DNA-binding small molecule drugs. Cancer Res 2018;78:1431–43.
35. Dermawan JK, Hitomi M, Silver DJ, Wu Q, Sandlesh P, Sloan AE, et al. Pharmacological targeting of the histone chaperone complex FACT preferentially eliminates glioblastoma stem cells and prolongs survival in preclinical models. Cancer Res 2016;76:2432–42.
36. Koman IE, Commane M, Paszkiewicz G, Hoonjan B, Pal S, Safina A, et al. Targeting FACT complex suppresses mammary tumorigenesis in Her2/neu transgenic mice. Cancer Prev Res (Phila) 2012;5:1025–35.
37. Dermawan JK, Gurova K, Pink J, Dowlati A, De S, Narla G, et al. Quinacrine overcomes resistance to erlotinib by inhibiting FACT, NF-kappaB, and cell-cycle progression in non-small cell lung cancer. Mol Cancer Ther 2014;13:2203–14.
38. Gasparian AV, Burkhart CA, Purmal AA, Brodsky L, Pal M, Saranadasa M, et al. Curaxins: anticancer compounds that simultaneously suppress NF-kappaB and activate p53 by targeting FACT. Sci Transl Med 2011;3:95ra74.
39. Bhakat KK, Sengupta S, Adeniyi VF, Roychoudhury S, Nath S, Bellot LJ, et al. Regulation of limited N-terminal proteolysis of APE1 in tumor via acetylation and its role in cell proliferation. Oncotarget 2016;7:22590–604.
40. Walther A, Johnstone E, Swanton C, Midgley R, Tomlinson I, Kerr D. Genetic prognostic and predictive markers in colorectal cancer. Nat Rev Cancer 2009;9:489.
41. van Triest B, Pinedo HM, van Hensbergen Y, Smid K, Telleman F, Schoenmakers PS, et al. Thymidylate synthase level as the main predictive parameter for sensitivity to 5-fluorouracil, but not for folate-based thymidylate synthase inhibitors, in 13 nonselected colon cancer cell lines. Clin Cancer Res 1999;5:643–54.
42. Sinicrope FA, Rego RL, Halling KC, Foster NR, Sargent DJ, La Plant B, et al. Thymidylate synthase expression in colon carcinomas with microsatellite instability. Clin Cancer Res 2006;12:2738–44.
43. Kakolyris S, Kaklamanis L, Engels K, Turley H, Hickson ID, Gatter KC, et al. Human apurinic endonuclease 1 expression in a colorectal adenoma-carcinoma sequence. Cancer Res 1997;57:1794–7.
44. Li M, Volker J, Breslauer KJ, Wilson DM 3rd. APE1 incision activity at abasic sites in tandem repeat sequences. J Mol Biol 2014;426:2183–98.
45. Lirussi L, Antoniali G, Vascotto C, D'Ambrosio C, Poletto M, Romanello M, et al. Nucleolar accumulation of APE1 depends on charged lysine residues that undergo acetylation upon genotoxic stress and modulate its BER activity in cells. Mol Biol Cell 2012;23:4079–96.
46. Charles Richard JL, Shukla MS, Menoni H, Ouararhni K, Lone IN, Roulland Y, et al. FACT assists base excision repair by boosting the remodeling activity of RSC. PLoS Genet 2016;12:e1006221.